

A neural model of discrete and continuous modes of visual discrimination

TOMMASO COSTA and MARIO FERRARO

Dipartimento di Fisica Sperimentale, Università di Torino, via Giuria 1, 10125 Torino, Italy

Received 19 December 1992; revised 29 April 1993; accepted 5 May 1993

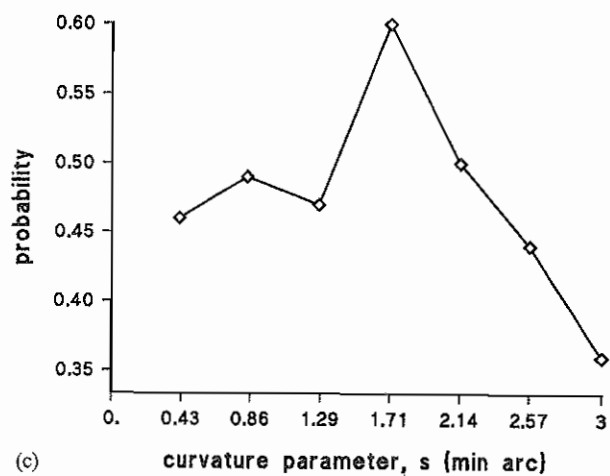
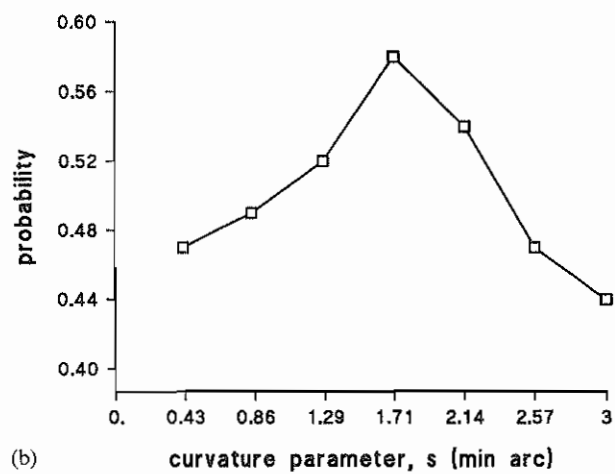
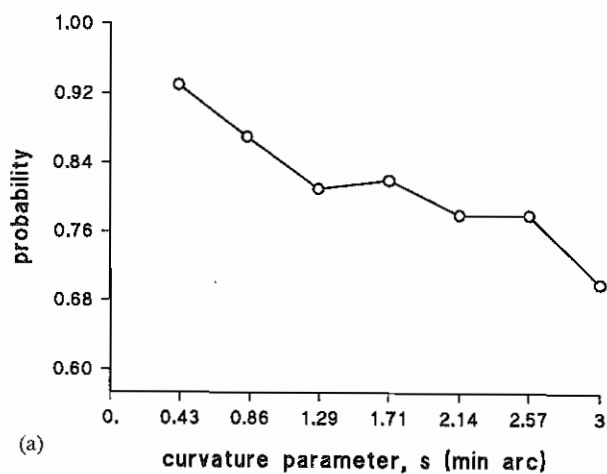
Abstract—A simple neural model of visual pattern discrimination is presented, based on the assumption that visual discrimination is determined by the differences in activity of a certain set of filters. These filters are the input units of a three-layer network. The units of the second layer have probabilities of activation that depend on the differences in activity of the input units and in turn they determine the probabilities of activation of a layer of output units from which probabilities of correct discrimination can be predicted. This model has been used to simulate discrete and continuous modes of curved-line discrimination and the results show good agreement with experimental data found in the literature.

1. INTRODUCTION

Data from several experimental paradigms show that visual discrimination performance by human observers can be associated with different types of encoding of the visual stimulus, termed *discrete* and *continuous* (Ferraro and Foster, 1984). When the stimulus duration is short, visual discrimination seems to be determined by a coarse, discrete encoding. Such performance has been reported in the discrimination of simple 3-dot figures (Foster, 1979, 1980) and in the discrimination of arrays of geometric elements (Beck and Ambler, 1972, 1973) and texture-like displays (Julesz, 1980). In contrast, when prolonged viewing is permitted, visual discrimination appears to be determined by smooth, continuous processes (Westheimer and McKee, 1977; Westheimer, 1979, 1981). These two different modes of visual encoding have also been observed in experiments on the discrimination of curved lines (Foster, 1983; Ferraro and Foster, 1986; Foster *et al.*, 1993).

In this paper we discuss a simple neural model which explains the occurrence of discrete and continuous modes of visual encoding; the results obtained by computer simulation are compared with data from discrimination experiments (Ferraro and Foster, 1986). In these experiments, the stimulus patterns were lines of different curvature drawn from a continuum generated by a 1-parameter transformation group, and curvature was specified by a parameter s which measured the distance between the chord and midpoint of the curved line. Each pattern display comprised three curved lines: two were identical, with curvature parameter $s - \Delta s$ (or $s + \Delta s$), and the third had curvature parameter $s + \Delta s$ (or, respectively, $s - \Delta s$); thus the patterns differed in parameter value by $2\Delta s$.

The subject's task was to identify the odd curve. Discrimination performance for these three-subpattern displays was measured for different display time courses: (1) 2-s display, no post-stimulus mask; (2) 100-ms display, no post-stimulus mask;



(3) 100-ms display, followed by a 100-ms blank field and then a random-line-segment masking field, duration 500 ms.

The results are shown in Fig. 1 for one subject, where the probability of correct discrimination is plotted as a function of the value of s (the *reference* value).

The empirical data show the existence of two extreme modes of discrimination, apparently controlled by stimulus duration: when the display duration is short, discrimination performance is characterized by a sharp peak at one point of the continuum, whereas for long display duration discrimination is characterized by a smooth, monotonic variation over the continuum (cf. Foster, 1983). These changes in performance can be ascribed to changes in the type of pattern representation assumed to be used by the visual system; a sharply peaked discrimination performance can be associated with the use of discrete encodings, and a smoothly varying discrimination can be associated with the use of continuous encodings. A theoretical rationale for this interpretation was given by Ferraro and Foster (1984, 1986).

2. THE MODEL

Consider a visual stimulus with intensity $I(x, y) \in \mathbf{R}$ (\mathbf{R} the real numbers) defined at each point (x, y) of the plane, and a filter \mathcal{F} operating on $I(x, y)$. Suppose that some activity r is generated by the filter in response to the stimulus. The response r is obtained by computing the filter's response at every point of the stimulus and by integrating the result over the stimulus domain (see Appendix). The set \mathcal{A} of the activities for different stimuli is a subspace of \mathbf{R} ; that is, \mathcal{F} projects the stimulus from physical space to a space of activities \mathcal{A} ; it is assumed that any further operation is carried out in \mathcal{A} . In particular, the discrimination of two stimulus patterns B_1, B_2 is then determined by their distance $|\delta r| = |r(B_1) - r(B_2)|$ in the activity space \mathcal{A} .

For the patterns of interest here, namely, curved lines, we have chosen the filter function as follows

$$\mathcal{F}(x, y) = -\nabla^2 G(x, y, \sigma_x, \sigma_y),$$

where

$$G(x, y, \sigma_x, \sigma_y) = \frac{1}{2\pi\sigma_x\sigma_y} \exp\left(\frac{-x^2}{2\sigma_x^2}\right) \exp\left(\frac{-y^2}{2\sigma_y^2}\right),$$

and ∇^2 is the Laplace operator $\left(\frac{\partial^2}{\partial^2x} + \frac{\partial^2}{\partial^2y}\right)$.

Thus

$$\mathcal{F}(x, y) = \frac{1}{2\pi\sigma_x\sigma_y} \left[\left(\frac{1}{\sigma_x^2} + \frac{1}{\sigma_y^2}\right) - \left(\frac{x^2}{\sigma_x^4} + \frac{y^2}{\sigma_y^4}\right) \right] \exp\left(\frac{-x^2}{2\sigma_x^2}\right) \exp\left(\frac{-y^2}{2\sigma_y^2}\right). \quad (1)$$

Figure 1. Curved-line discrimination performance. The proportion of correct discriminations of curved lines differing by parameter value $2\Delta s$ is plotted as a function of the reference value s . The three stimulus time courses were (a) 2-s display, no post-stimulus mask; (b) 100-ms display, no post-stimulus mask; (c) 100-ms display, followed by a random line-segment mask.

A similar filter function was used in a previous study (Wilson, 1985) of curvature discrimination.

Next we assume that pattern encoding can be thought of as a dynamical process that in a time-interval Δt does a sampling of the stimulus (Massaro, 1975; Lupker and Massaro, 1979). The notion that the visual system performs sampling is supported by psychophysical and physiological data (Reed, 1973; Wilson *et al.*, 1990). The number of elements in the sample depends on the display duration: for a short display duration, only a few sampling operations are possible and the number of sampled elements will be small; if prolonged viewing is permitted, the sample will represent virtually all of the elements of the original stimulus. In the present case,

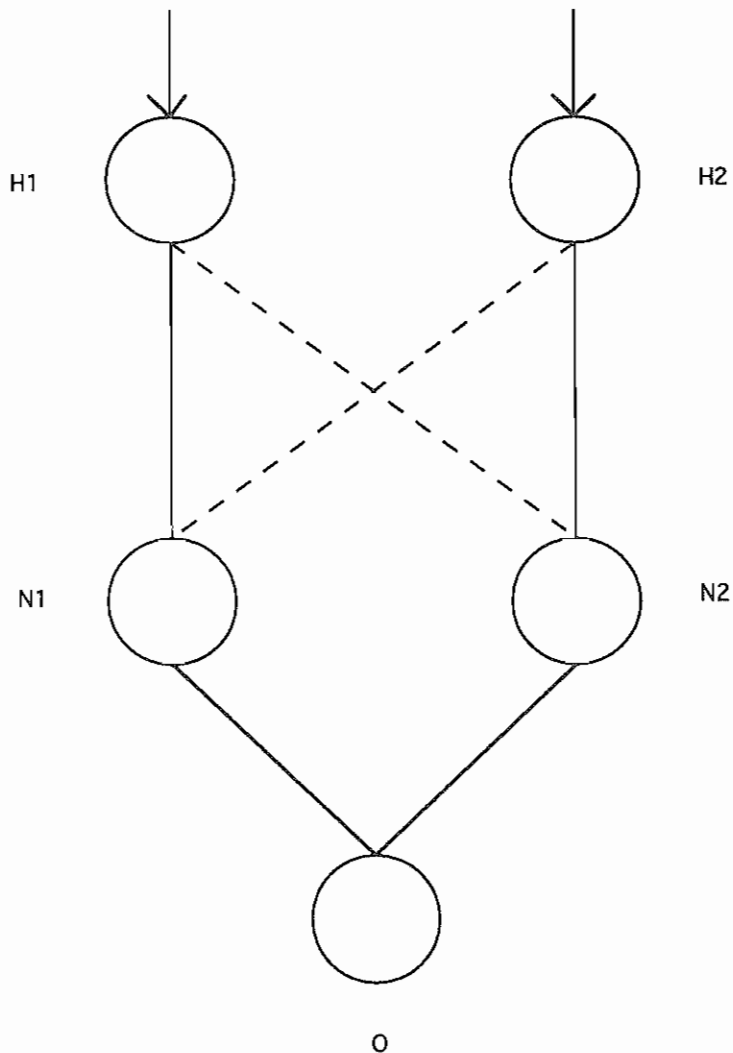


Figure 2. Neural network architecture. Excitatory and inhibitory connections are represented by continuous and broken lines respectively.

this implies that the curved lines forming the stimulus pattern are supposed to be sampled with various degrees of fineness depending on the duration of the stimulus.

In the model presented here it is assumed that discrimination of patterns depends on the differences of the response of a given filter to the different patterns, or, equivalently, on the differences of activity of units having the same filter function and operating on different patterns. To perform a discrimination, a neural system must be able to compute the difference between the responses of such units.

A diagram of such a system is shown, for two patterns, in Fig. 2. Suppose we are given two patterns B_1, B_2 ; let r_1, r_2 be the responses of the units $\mathcal{H}_1, \mathcal{H}_2$. Further let us assume that $\mathcal{H}_1, \mathcal{H}_2$ have excitatory connections to two hidden units $\mathcal{N}_1, \mathcal{N}_2$ respectively, and inhibitory connections to $\mathcal{N}_2, \mathcal{N}_1$ respectively. The activity of the units \mathcal{N}_i is all-or-none, and the probability that \mathcal{N}_i is active depends on the total input $r_i - r_j$, $i, j = 1, 2, i \neq j$. We define the probability thus

$$p_i = \begin{cases} [1 + \exp(-\beta(r_i - r_j) + \alpha)]^{-1}, & \text{if } r_i > r_j, \\ 0, & \text{if } r_i \leq r_j. \end{cases} \quad (2)$$

The probability p_i is therefore a sigmoidal function of the difference $r_i - r_j$; the parameter α is the value of $r_i - r_j$ where the sigmoid has an inflexion point; and β is the slope of the function at this point (Hertz *et al.*, 1991). Note that the definition of p_i implies that \mathcal{N}_1 and \mathcal{N}_2 cannot be active simultaneously, and that both \mathcal{N}_1 and \mathcal{N}_2 are inactive if $r_1 = r_2$. Finally we introduce an output unit O which has an excitatory connection with both \mathcal{N}_1 and \mathcal{N}_2 , and zero threshold. Discrimination occurs when $O = 1$, that is, the unit O is active, and this occurs only if $|r_1 - r_2| > 0$. Then it is clear from Eqn (2) that the probability of activation of O , and hence the probability of discrimination, is

$$P_d = \begin{cases} [1 + \exp(-\beta|\delta r| + \alpha)]^{-1}, & \text{if } |\delta r| > 0, \\ 0, & \text{if } |\delta r| = 0, \end{cases} \quad (3)$$

where $|\delta r| = |r_1 - r_2|$. It is obvious that the probability P_d is an increasing function of $|\delta r|$.

Let us now consider the task of detecting an odd pattern among $n - 1$ other identical patterns. In this case, n units $\mathcal{H}_1, \mathcal{H}_2, \dots, \mathcal{H}_n$ are necessary, and, since there are $n(n - 1)/2$ differences in activity, $n(n - 1)$ units $\mathcal{N}(i, j)$ in the hidden layer are needed, each of which receives an excitatory input from \mathcal{H}_i and an inhibitory input from \mathcal{H}_j . In the output layer, there are $n(n - 1)/2$ output units $O_{ij} = O_{ji}$ with $i \neq j$. If B_k is the pattern to be discriminated, the configuration of the output units O_{ij} that corresponds to a correct discrimination is defined by $O_{ik} = 1$ and $O_{ij} = 0$ if $i, j \neq k$; that is, discrimination is correct when the only units that are active are precisely the units O_{ik} which respond to the difference in activity between \mathcal{H}_k and the other input units $\mathcal{H}_i, i \neq k$. The probability that O_{ij} is active ($O_{ij} = 1$) is given by

$$P(i, j) = \begin{cases} [1 + \exp(-\beta|\delta r(i, j)| + \alpha)]^{-1}, & \text{if } |\delta r(i, j)| > 0, \\ 0, & \text{if } |\delta r(i, j)| = 0, \end{cases} \quad (4)$$

where $|\delta r(i, j)| = |r_i - r_j|$. Suppose $i, j \neq k$; then $B_i = B_j$, and $r_i = r_j$. From Eqn (4) it follows that $P(i, j) = 0$, that is, $O_{ij} = 0$ with probability 1. The probability of correct

discrimination P_d is

$$P_d = \prod_{i \neq k} P(i, k). \quad (5)$$

Consider the case $n = 3$ and let us assume that the odd pattern is B_1 . Then the configuration of the output units corresponding to a correct discrimination is $O_{12} = O_{13} = 1$, $O_{23} = 0$, and its probability is

$$P_d = P(1, 2)P(1, 3). \quad (6)$$

3. COMPUTATIONAL PROCEDURE

3.1. Continuous mode

For long display durations, the continuous mode of encoding can be simulated by considering just the responses of the filter to each curved line.

The curved lines used in this simulation were produced, as in Ferraro and Foster (1986), by fixing the two terminal members of the range and generating intermediate members by the action of a 1-parameter transformation group, in this case a process of horizontal scaling. As mentioned earlier, curvature was specified by the parameter s measuring the distance between the midpoint of the chord, whose length l was kept constant, and the midpoint of the curved line. The range of the continuum, the dimension of the curved lines and value of Δs were the same as in Ferraro and Foster (1986). In polar coordinates a point $P(x, y)$ on a curved line, centred at the origin and characterized by a parameter value s , is given by

$$\begin{aligned} x &= \rho(s) \cos \theta, \\ y &= \rho(s) \sin \theta, \end{aligned}$$

where

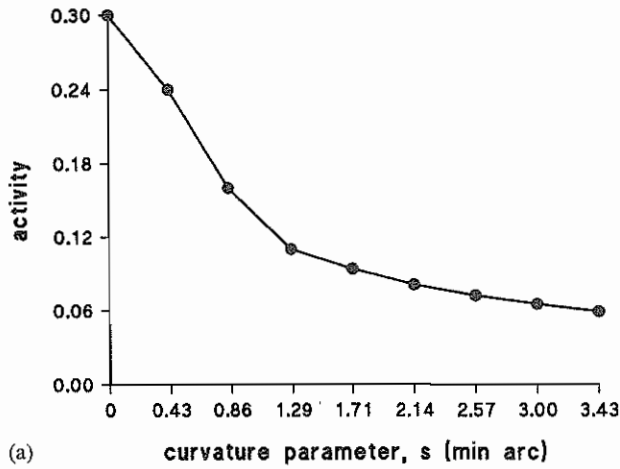
$$\rho(s) = \frac{((l/2)^2 + s^2)}{2s},$$

and $-\theta_0 \leq \theta \leq \theta_0$, $\theta_0 = \arcsin\left(\frac{l}{2\rho(s)}\right)$.

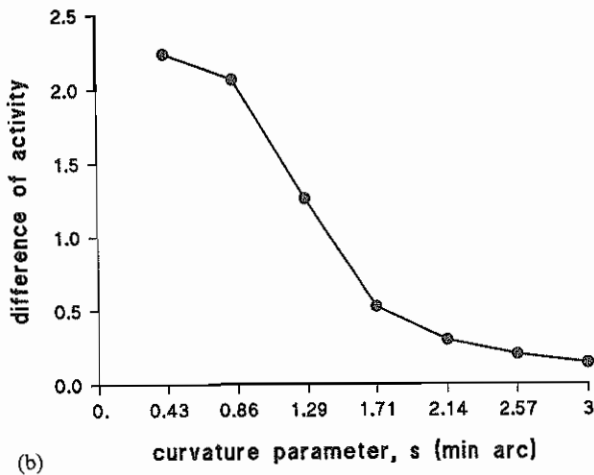
The response r of the filter \mathcal{F} was obtained by computing its convolution with the line and integrating the result, as shown in the Appendix. Thus

$$\begin{aligned} r(s) &= \frac{1}{2\pi\sigma_x\sigma_y} \int_{-\theta_0}^{\theta_0} \exp\left(\frac{-\rho^2(s) \cos^2 \theta}{2\sigma_x^2}\right) \exp\left(\frac{-\rho^2(s) \sin^2 \theta}{2\sigma_y^2}\right) \\ &\quad \left[\left(\frac{1}{\sigma_x^2} + \frac{1}{\sigma_y^2} \right) - \left(\frac{\rho^2(s) \cos^2 \theta}{\sigma_x^4} + \frac{\rho^2(s) \sin^2 \theta}{\sigma_y^4} \right) \right] \rho d\theta \end{aligned} \quad (7)$$

Note that r is a function of the parameter s . Figure 3a shows this dependence on s , and Fig. 3b shows the differences in activity $\delta r(s) = r(s - \Delta s) - r(s + \Delta s)$ for lines with parameter values $s - \Delta s$, $s + \Delta s$, as a function of the reference value s . Here, and in all subsequent computations, the space constants $\sigma_x = 0.8$ arcmin, $\sigma_y = 9$ arcmin.



(a)



(b)

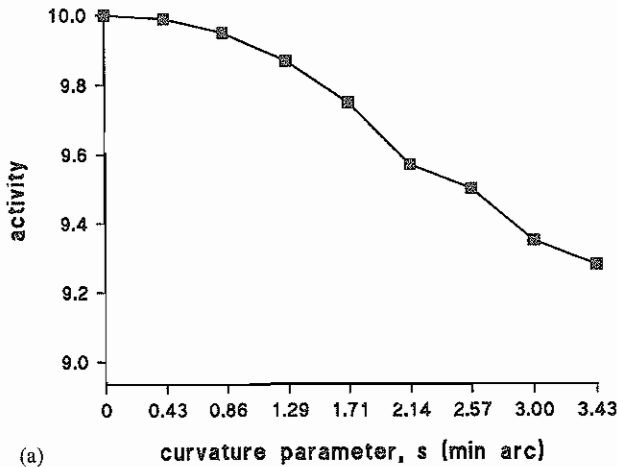
Figure 3. (a) Activity of the filter \mathcal{F} , as defined by Eqn (7), for curved lines with different values of curvature parameter s . Activity values are expressed in arbitrary units. (b) Differences in activity of the filter for curves differing by parameter value $2\Delta s$ plotted against the reference value s .

3.2. Discrete mode

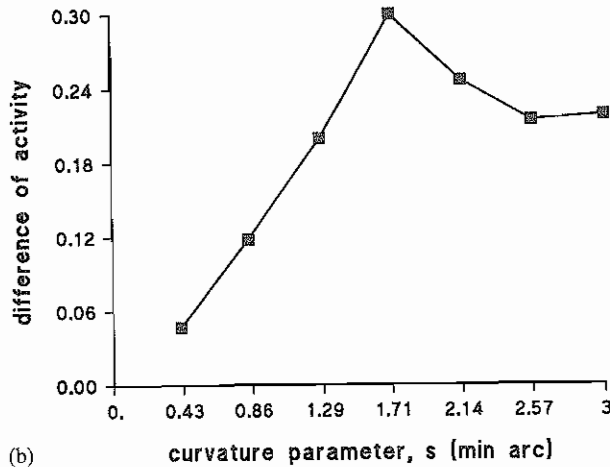
It was suggested earlier that during brief displays only a relatively small number of points are sampled by the visual system. To simulate this effect the curved lines were sampled on a discrete 51×51 grid. The activity of the filter was computed using a discretized version of (7):

$$r(s) = \sum_{-i}^i \sum_{-j}^j \mathcal{F}_d(i, j) I_d(x_0 + i, y_0 + j), \quad (8)$$

where $\mathcal{F}_d(i, j)$ and $I_d(i, j)$ are the discretized versions of the filter and the image



(a)



(b)

Figure 4. (a) Activity of the filter \mathcal{F}_a , operating on a discretized version of the curves, for different values of the curvature parameter s (see Eqn (8)). Activity values are expressed in arbitrary units. (b) Differences in activity of the filter for curves differing by parameter value $2\Delta s$ plotted against the reference value s .

respectively, and x_0, y_0 are the coordinates of the image centre. Figure 4(a, b) shows the activities and difference in activities in this case.

It is well known that a post-stimulus mask interrupts the processing of a visual stimulus (Reed, 1973), effectively reducing the time during which sampling can be performed. The effect of a mask in the curvature-discrimination experiments (Ferraro and Foster, 1986) was simulated by deleting randomly some of the points forming the discrete image. The activities were computed by averaging the results of 100 individual simulations. Activities and differences in activities are shown in Figs 5 (a, b).

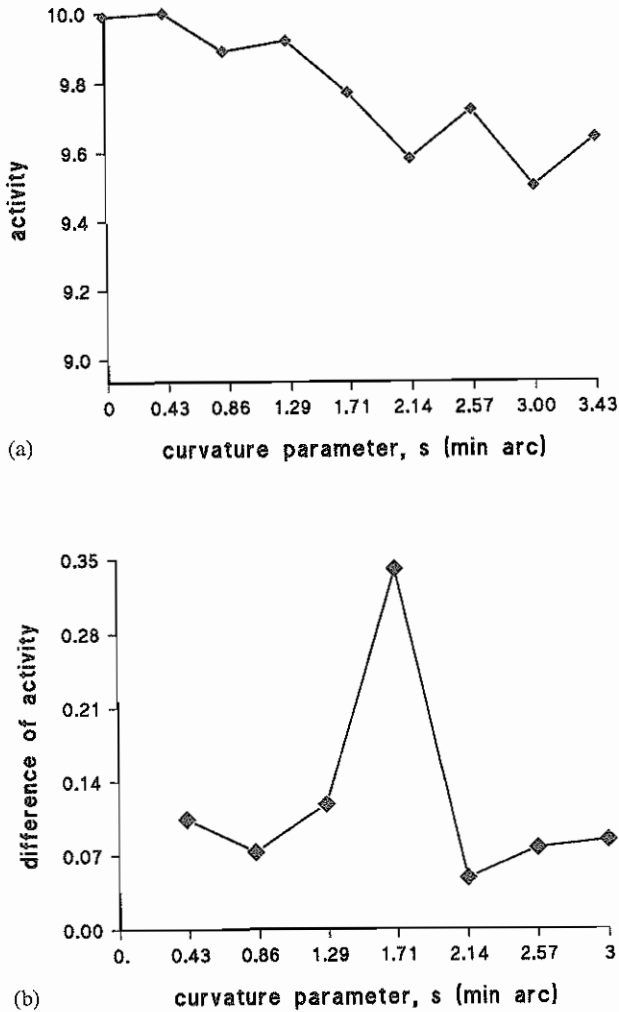


Figure 5. (a) Activity of the filter \mathcal{F}_d , as defined by Eqn (8), with some points of the discretized version of the curve randomly deleted, for different values of the curvature parameter s . Activity values are expressed in arbitrary units. (b) Differences in activity of the filter for curves differing by parameter value $2\Delta s$ plotted against the reference value s . The results were obtained by averaging over 100 individual simulations.

4. RESULTS AND DISCUSSION

To compare the predictions of the model with the results of experiment, Eqn (6) must be modified to take into account the fact that the experiments were performed with a forced-choice paradigm in which correct discrimination could arise also by chance. The total probability of correct discrimination P_t can be computed as follows. Suppose that B_1 is the odd pattern, then $O_{23} = 0$ with probability 1. Correct discrimination occurs with probability 1 when $O_{12} = O_{13} = 1$, and this event has probability $P_d = P(1, 2)P(1, 3)$, as shown in Eqn (6). If the event $O_{12} = O_{13} = 0$ occurs, which has probability $(1 - P(1, 2))(1 - P(1, 3))$, the odd pattern is selected randomly among B_1, B_2, B_3 and the probability of correct recognition is, in this case, $1/3$.

Table 1

Estimates of the model parameters and goodness of fit for the three timing conditions

Parameter	2 s	100 ms	100-ms masking
β	0.56	2.76	3.9
α	-0.89	1.08	1.26
χ^2_ν	1.14	0.82	1.45
P	> 0.3	> 0.5	> 0.2

Finally, for $O_{12} = 1, O_{13} = 0$, the probability is $P(1,2)(1 - P(1,3))$, and for $O_{12} = 0, O_{13} = 1$, the probability is $P(1,3)(1 - P(1,2))$. In this case it is assumed that the odd subpattern is selected by means of a random choice between B_1 and B_2 or between B_1 and B_3 , respectively. Then the total probability of correct discrimination is given by

$$P_t = P_d + \frac{1}{2}P(1,2)(1 - P(1,3)) + \frac{1}{2}P(1,3)(1 - P(1,2)) + \frac{1}{3}(1 - P(1,2))(1 - P(1,3)) \quad (9)$$

This probability function contains two free parameters β and α (from Eqn (2)); they were determined with standard chi-square techniques by minimizing

$$\chi^2_\nu = \frac{1}{\nu} \sum_{i=1}^n \frac{(f_i - P_t(i))^2}{\sigma_i^2},$$

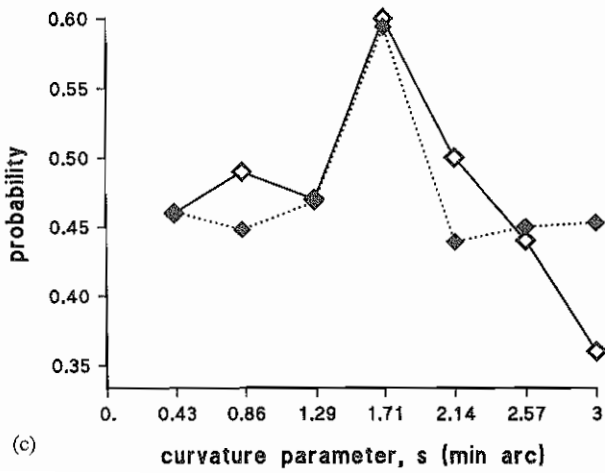
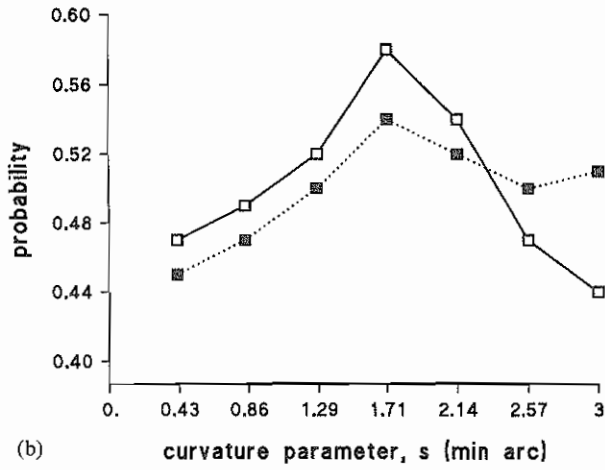
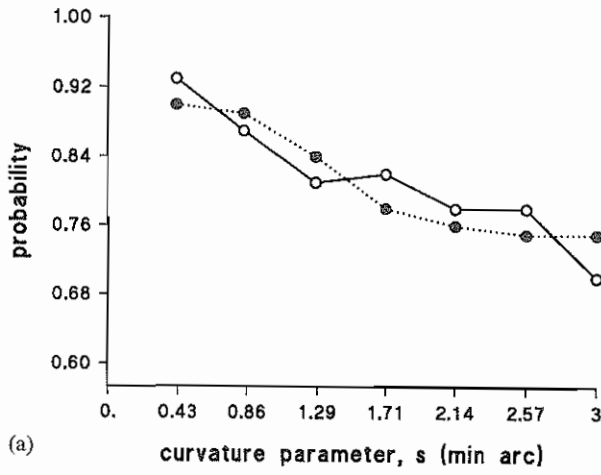
where f_i and $P_t(i)$ are the experimental and predicted discrimination probabilities, $n = 7$ is the number of experimental points, $\nu = n - m$ is the number of degrees of freedom, $m = 2$ is the number of parameters to be determined, and the σ_i are the standard errors of the experimental distribution.

The results are shown in Table 1, where P is the level of significance of the fit.

The predicted discrimination performances for the three different conditions are shown, together with the experimental curves, in Fig. 6(a-c). The simulations show good agreement between experimental and predicted values of discrimination performance, suggesting that a mechanism similar to that presented here may be used by the visual system in simple discrimination tasks.

The basic assumption of the model is that a stimulus pattern can be represented as a point in the activity space \mathcal{A} of a filter, or, more generally, of a set of filters. It follows that, with an appropriate choice of filter function, a given feature can be coded by the filter's activity, and discriminability of patterns is then determined by differences in activity. In the present case, curved lines characterized by different values of the curvature parameter s are encoded by the outputs of the filter \mathcal{F} defined by Eqn (1). For long display durations the activity of the filter is a monotonic, smooth function of s . Thus different values of activity continuously encode the parameter curvature s . In contrast, for short display durations with a mask, the activity appears to fluctuate around a high level for $s < s_0$ and around a relatively low level for $s > s_0$,

Figure 6. Comparisons between experimental data (open symbols) and data predicted by the model (filled symbols). (a) 2-s display; (b) 100-ms display, no post-stimulus mask; (c) 100-ms display, followed by a random line-segment mask. See text for explanation.



$s_0 = 1.71$ arcmin, and the resulting encoding of the curved lines is constrained to two categories only.

The contrast between these two extreme types of activity becomes more apparent if one considers the difference in activities $\delta r(s) = r(s - \Delta s) - r(s + \Delta s)$: for long display durations δr is a smooth and monotonic function of s , whereas for short display durations with a mask δr is characterized by a sharp peak at s_0 ; for short display durations without a mask the dependence of δr on s is of intermediate form. Because of the excitatory and inhibitory connections of the filters with the hidden units $\mathcal{N}(i, j)$, the probability of activation of these units depends on the differences in activity between pairs of filters, and the output units simply register the activity of the units $\mathcal{N}(i, j)$. Thus it is clear that the discrimination performance of the network is determined by the activity differences δr and that the qualitative behaviour of the probabilities of correct discrimination does not depend on β and α or on the specific form of the probability function given in Eqn (2); in fact it is easy to prove that any probability which is a monotonic function of $|r_i - r_j|$ will give rise to similar trends.

It must be noted, however, that different experimental conditions correspond to different values of the parameters β and α of the probability function, and this suggests that even though activity differences of the filter determine discriminability the observed discrimination performance is influenced by other factors.

The model which has been presented here to simulate continuous and discrete modes of visual discrimination of curved lines can, with an appropriate set of filters, be used to simulate the visual encoding and discrimination of other classes of simple stimuli. This model can furthermore be extended, apart from some technical difficulties, to deal with the encoding of more complex stimuli, characterized by several features. Each feature can be thought of as being coded by an appropriate filter and the discriminability determined by a distance function in a suitable multi-dimensional activity space.

Acknowledgements

We thank David Foster and the reviewers for their critical reading of the manuscript and many valuable suggestions.

REFERENCES

- Beck, J. and Ambler, B. (1972). Discriminability of differences in line slope and in line arrangement as a function of mask delay. *Percept. Psychophys.* **12**, 33–38.
- Beck, J. and Ambler, B. (1973). The effects of concentrated and distributed attention on peripheral acuity. *Percept. Psychophys.* **14**, 225–230.
- Ferraro, M. and Foster, D. H. (1984). Characterization of discrete and continuous modes of visual pattern discrimination. *Biol. Cybernet.* **50**, 9–13.
- Ferraro, M. and Foster, D. H. (1986). Discrete and continuous modes of curved-line discrimination by effective stimulus duration. *Spatial Vision* **1**, 219–230.
- Foster, D. H. (1979). Discrete internal pattern representation and visual detection of small changes in pattern shape. *Percept. Psychophys.* **26**, 459–468.
- Foster, D. H. (1980). A spatial perturbation technique for the investigation of discrete internal representation of visual patterns. *Biol. Cybernet.* **38**, 159–169.
- Foster, D. H. (1983). Visual discrimination, categorical identification, and categorical rating in brief displays of curved lines: implications for discrete encoding processes. *J. Exp. Psychol.: Human Percept. Perform.* **9**, 785–806.
- Foster, D. H., Simmons, D. R. and Cook, M. J. (1993). The cue for contour-curvature discrimination. *Vision Res.* **33**, 329–341.

Hertz, J., Krogh, A. and Palmer, R. G. (1991). *Introduction to the Theory of Neural Computation*. Addison-Wesley, Redwood City, CA.

Julesz, B. (1980). Spatial nonlinearities in the instantaneous perception of textures with identical power spectra. *Phil. Trans. R. Soc. Lond.* **B290**, 83–94.

Lupker, S. J. and Massaro, D. W. (1979). Selective perception without confounding contributions of decision and memory. *Percept. Psychophys.* **25**, 60–69.

Massaro, D. W. (1975). *Experimental Psychology and Information Processing*. Rand McNally, Chicago, IL.

Reed, S. K. (1973). *Psychological Processes in Pattern Recognition*. Academic Press, New York.

Rosenfeld, A. and Kak, A. C. (1982). *Digital Picture Processing*. Academic Press, Orlando, FL.

Westheimer, G. (1979). The spatial sense of the eye. *Invest. Ophthalmol. Visual Sci.* **18**, 893–912.

Westheimer, G. (1981). Visual hyperacuity. *Prog. Sensor. Physiol.* **1**, 1–30.

Westheimer, G. and McKee, S. P. (1977). Spatial configuration for visual hyperacuity. *Vision Res.* **17**, 941–947.

Wilson, H. R. (1985). Discrimination of contour curvature: data and theory. *J. Opt. Soc. Am.* **A2**, 1191–1198.

Wilson, H. R., Levi, D., Maffei, L., Rovamo, J. and DeValois, R. (1990). The perception of the form: retina to striate cortex. In: *Visual Perception. The Neurophysiological Foundations*. L. Spillmann and J. S. Werner (Eds). Academic Press, San Diego, CA.

APPENDIX

Consider a bright curved line against a dark background. Let $\gamma(t) = (\alpha(t), \beta(t))$, $t \in [a, b]$, be a parameterization of the curve; then $x = \alpha(t)$, $y = \beta(t)$ are the coordinates of the points of the line. The light intensity of any point $p(t) = (\alpha(t), \beta(t))$ can be expressed as $\delta(x - \alpha(t), y - \beta(t))$, where δ is the Dirac delta function (Rosenfeld and Kak, 1982). Let \mathcal{F} be a filter. The response r of the filter to a curved line is obtained by computing the response of \mathcal{F} to each point on the line and by integrating all those responses along the line. Formally, this operation corresponds to a convolution of \mathcal{F} with $\delta(x - \alpha(t), y - \beta(t))$ followed by an integration along γ . The activity of the filter is thus

$$\begin{aligned}
 r &= \int_{\gamma} d\tau \iint \mathcal{F}(x, y) \delta(x - \alpha(\tau), y - \beta(\tau)) dx dy \\
 &= \int_{\gamma} \mathcal{F}(\alpha(\tau), \beta(\tau)) d\tau \tag{A1} \\
 &= \int_{\gamma} \mathcal{F}(\alpha(t), \beta(t)) \sqrt{\dot{\alpha}^2(t) + \dot{\beta}^2(t)} dt,
 \end{aligned}$$

where τ is the arclength, and $d\tau = \sqrt{\dot{\alpha}^2(t) + \dot{\beta}^2(t)} dt$.

Suppose that \mathcal{F} has the form given in Eqn (1) and that the parameterization of the line is $x = \rho \cos \theta$ and $y = \rho \sin \theta$, where ρ is constant for any given curve, and $[a, b] = [-\theta_0, \theta_0]$. Then, $d\tau = \rho dt$ and the response of the filter is given by

$$\begin{aligned}
 r &= \frac{1}{2\pi\sigma_x\sigma_y} \int_{-\theta_0}^{\theta_0} \exp\left(\frac{-\rho^2 \cos^2 \theta}{2\sigma_x^2}\right) \exp\left(\frac{-\rho^2 \sin^2 \theta}{2\sigma_y^2}\right) \\
 &\quad \left[\left(\frac{1}{\sigma_x^2} + \frac{1}{\sigma_y^2}\right) - \left(\frac{\rho^2 \cos^2 \theta}{\sigma_x^4} + \frac{\rho^2 \sin^2 \theta}{\sigma_y^4}\right) \right] \rho d\theta. \tag{A2}
 \end{aligned}$$

6

7

8

9

10